Elsevier Editorial System(tm) for Mechanisms of Development

Manuscript Draft

Manuscript Number: MOD-1212R4

Title: Thyroid development in zebrafish lacking TAZ.

Article Type: Full Length Article

Keywords: Taz, wwtr1, thyroid, follicle, organ size, zebrafish.

Corresponding Author: Dr. Paolo Sordino, Ph.D.

Corresponding Author's Institution: Stazione Zoologica Anton Dohrn

First Author: Andrea Pappalardo, Ph.D.

Order of Authors: Andrea Pappalardo, Ph.D.; Immacolata Porreca, Ph.D.; Luigi Caputi, Ph.D.; Elena De Felice, Ph.D.; Stephan Schulte-Merker, Ph.D.; Mariastella Zannini, Ph.D.; Paolo Sordino, Ph.D.

Abstract: TAZ is a signal-responsive transcriptional coregulator implicated in several biological functions, from chondrogenesis to regulation of organ size. Less well studied, however, is its role in thyroid formation. Here, we explored the in vivo effects on thyroid development of morpholino (MO)-mediated knockdown of wwtr1, the gene encoding zebrafish Taz. The wwtr1 gene is expressed in the thyroid primordium and pharyngeal tissue of developing zebrafish. Compared to mammalian cells, in which TAZ promotes expression of thyroid transcription factors and thyroid differentiation genes, wwtr1 MO injection in zebrafish had little or no effect on the expression of thyroid transcription factors, and differentially altered the expression of thyroid differentiation genes. Analysis of wwtr1 morphants at later stages of development revealed that the number and the lumen of thyroid follicles, and the number of thyroid follicle cells, were significantly smaller. In addition, TAZ-depleted larvae displayed patterning defects in ventral cranial vessels that correlate with lateral displacement of thyroid follicles. These findings indicate that the zebrafish Taz protein is needed for the normal differentiation of the thyroid and are the first to suggest that TAZ confers growth advantage to the endocrine gland.

Naples, October 12 2015

Dear Editor,

on behalf of my collaborators, I wish to thank you for reviewing our manuscript "Thyroid development in zebrafish lacking TAZ" that we submitted for publication considerations to *Mechanisms of Development*. We greatly appreciated the comments of reviewers, who gave us the opportunity to further improve our work. In this resubmission, we included percentage of 4 dpf *wwtr1* knockdown larvae showing displacement of thyroid follicles, replaced one reference, and amended the manuscript according to all concerns raised during the reviewing process. We hope that the edited version of our manuscript may be now considered acceptable for publication and we look forward to hearing from you.

Sincerely,

Paolo Sordino

***Revision Notes**

Reviewers' comments:

Reviewer #1: Minor comments

on page 6 : « Zebrafish wwtr1 transcription in the thyroid was further supported by the observation of follicles immunoreactive for thyroglobulin in the pharyngeal domain of wwtr1 expression (Fig. 2O, O'). » There is no Fig. 2O' in my copy and no thyroid in Fig. 2O. Reference to Fig. 2N??? Same mistake is present in the legend to Figure 2.

on page 6: "At 4 dpf, wwtr1 expression is detected in brain, liver, gut, pectoral fins (stronger proximal), and cartilage elements of the craniofacial (branchial arches) and neurocranial (ethmoid plate and trabeculae) areas (Fig. 2P-S)." Reference to Fig. 2O-S ???

We amended the Results text and Fig. 2 legend accordingly.

The authors should consider changing the term "territories" throughout the MS when referring to sites of TAZ expression. Change to "tissues" or "expression domains".

We amended the text accordingly.

on page 7: "At 5 dpf, loss of thyroid follicles was less pronounced (26,2%) and not statistically supported (p > 0.01) (Tab. 1)." "loss of thyroid follicles" is probably not adequate here as the tissue is not lost. "Difference in detectable follicles" or similar might be better to describe the observations.

We amended the text accordingly.

Figure legends:

My copy has no asterisk in Figure 2B.

The asterisk mentioned in Fig. 3 legend referred to a previous submission. The sentence was removed. Moreover, in accordance with Fig. 2 legend we added arrowhead in Fig. 2O and P to point to higher expression in pectoral fins proximally.

Reviewer #2: In the revised version of the manuscript, the authors focus on the thyroid phenotype in TAZ knockdown zebrafish. These data are well documented. The influence of TAZ knockdown on vascular patterning is not mentioned in the abstract anymore. This part, if to be included in the manuscript, needs further clarification.

Accordingly, we added to the Abstract a sentence on the association between abnormal vessel patterning and follicle displacement. However, we have not investigated the molecular mechanism underpinning these two phenotypes, for example to test the hypothesis of a direct role of TAZ in blood vessel formation.

Papparlado et al. aim to understand "whether follicle positioning was influenced by wwtr1 knockdown specific vascular malformations." They show that the patterning of the vasculature was severely affected in wwtr1 morphants. However, they not provide quantifications of the observed vascular phenotypes. For example, do they always observe failure of ventral aorta fusion into a midline channel? The conclusion of section 2.5 is not clear, since not quantified either. The authors conclude that thyroid follicles…"occasionally were not associated with the ventral aorta." The authors need to quantify this statement, e.g. in how many embryos do they observe the ectopically positioned thyroid follicles in comparison to wildtype embryos?

We amended the text accordingly by writing that all wwtr1 MO-injected tg(kdr-like:gfp) (100%) larvae analyzed in this work (n=14) showed lack of ventral aorta fusion. We also included the percentage of TAZ morphant larvae showing ectopic thyroid follicles at the beginning of section 2.5.

The observations are correlative at this point. There are blood vessel defects in taz morphants and there are defects in thyroid follicle positioning. However, it is not clear if the mispatterned blood vessels lead to the thyroid positioning defects. The authors should acknowledge this fact, in particular in the discussion, point "3.3 Abnormal blood vessel morphology causes thyroid follicle displacement". This section has a misleading title that is not supported by the findings. The results only state (point 2.5) that "Taz depletion causes alteration of blood vessel patterning".

Although the displacement of thyroid follicles as a consequence of blood vessel mispatterning has already been demonstrated (Alt et al., 2006b; Fagman et al., 2004, 2006; Opitz et al., 2011, 2012), we agree with Reviewer 2 about the misleading title of section 3.3 (when taking in consideration our data set) and changed it accordingly.

Minor

The authors cite Anderson et al. (2008) in the discussion, quoting that "TAZ exerts a role in blood vessel fusion through direct regulation of TGFb signaling downstream factors." The cited manuscript describes the phenotype of loss of function of unc45a, a myosin chaperone, on vascular development and does not mention TGFb signaling downstream factors.

We eliminated the wrong citation of Anderson et al. 2008.

Another reviewer asked for a reference for the in vivo demonstration of TAZ interaction with Pax8 and TTF-1. The authors did not correct this statement in the discussion (page 10, top).

We amended the text accordingly.

Abstract

TAZ is a signal-responsive transcriptional coregulator implicated in several biological functions, from chondrogenesis to regulation of organ size. Less well studied, however, is its role in thyroid formation. Here, we explored the *in vivo* effects on thyroid development of morpholino (MO)-mediated knockdown of *wwtr1*, the gene encoding zebrafish Taz. The *wwtr1* gene is expressed in the thyroid primordium and pharyngeal tissue of developing zebrafish. Compared to mammalian cells, in which TAZ promotes expression of thyroid transcription factors and thyroid differentiation genes, *wwtr1* MO injection in zebrafish had little or no effect on the expression of thyroid transcription factors, and differentially altered the expression of thyroid differentiation genes. Analysis of *wwtr1* morphants at later stages of development revealed that the number and the lumen of thyroid follicles, and the number of thyroid follicle cells, were significantly smaller. In addition, TAZ-depleted larvae displayed patterning defects in ventral cranial vessels that correlate with lateral displacement of thyroid follicles. These findings indicate that the zebrafish Taz protein is needed for the normal differentiation of the thyroid and are the first to suggest that TAZ confers growth advantage to the endocrine gland.

***Highlights**

- The zebrafish *wwtr1* gene is expressed in the developing thyroid.
- Loss of Taz by morpholino-based knockdown alters the expression of thyroid differentiation genes in zebrafish
- Zebrafish Taz has a positive role in thyroid morphogenesis and growth.

*Manuscript
Click here to view linked References

Thyroid development in zebrafish lacking Taz.

Andrea Pappalardo[a,b,1], Immacolata Porreca[c,d,1], Luigi Caputi[c], Elena De Felice[c,], Stephan Schulte-Merker[e], Mariastella Zannini[a], Paolo Sordino[c,*]

[a] Institute of Experimental Endocrinology and Oncology 'G. Salvatore' - CNR, 80131 Naples, Italy.

[b] IRCCS Fondazione Stella Maris, 56018 Calambrone, Pisa, Italy.

[c] Stazione Zoologica Anton Dohrn, 80121 Naples, Italy.

[d] IRGS, Biogem, 83031 Ariano Irpino, Avellino, Italy.

[e] Hubrecht Institute-KNAW and University Medical Centre, 3584 CT Utrecht, The Netherlands.

[1] These authors contributed equally to this work.

* Corresponding author. Stazione Zoologica Anton Dohrn, Villa Comunale, 80121 Naples, Italy. Phone: +39 081 5833283, Fax: +39 081 7641355, *E-mail address*: paolo.sordino@szn.it (P. Sordino).

Abstract

TAZ is a signal-responsive transcriptional coregulator implicated in several biological functions, from chondrogenesis to regulation of organ size. Less well studied, however, is its role in thyroid formation. Here, we explored the *in vivo* effects on thyroid development of morpholino (MO)-mediated knockdown of *wwtr1*, the gene encoding zebrafish Taz. The *wwtr1* gene is expressed in the thyroid primordium and pharyngeal tissue of developing zebrafish. Compared to mammalian cells, in which TAZ promotes expression of thyroid transcription factors and thyroid differentiation genes, *wwtr1* MO injection in zebrafish had little or no effect on the expression of thyroid transcription factors, and differentially altered the expression of thyroid differentiation genes. Analysis of *wwtr1* morphants at later stages of development revealed that the number and the lumen of thyroid follicles, and the number of thyroid follicle cells, were significantly smaller. In addition, TAZ-depleted larvae displayed patterning defects in ventral cranial vessels that correlate with lateral displacement of thyroid follicles. These findings indicate that the zebrafish Taz protein is needed for the normal differentiation of the thyroid and are the first to suggest that TAZ confers growth advantage to the endocrine gland.

Keywords: Taz, *wwtr1*, thyroid, follicle, organ size, zebrafish.

1. Introduction

TAZ (Transcriptional co-Activator with PDZ binding motif), also referred to as Wwtr1 (WW-domain containing transcription regulator 1), is a transcriptional coactivator highly expressed in kidney, heart, lung, liver, testis, and placenta (Kanai et al., 2000). The TAZ protein is characterized by a central WW-domain that mediates protein-protein interaction, followed by a highly conserved C-terminal sequence containing a coiled-coil domain that recruits core components of the transcriptional machinery. In addition, TAZ contains a PDZ binding motif at its C-terminus, required for the transcriptional coactivator activity and that promotes TAZ nuclear localization to discrete foci, and a 14-3-3 binding motif within the conserved N-terminal portion (Kanai et al., 2000; Kodaka and Hata, 2014). TAZ uses different binding partners to activate distinct sets of transcriptional targets, suggesting that it may be involved in several biological processes (Wang et al., 2009; Hong and Guan, 2012; Piccolo et al., 2014). Among TAZ functions are the roles in cell migration and proliferation, invasion in breast cancer cells, molecular rheostat in mesenchymal stem cells (MSC) and organ size control (Saucedo and Edgar, 2007; Zhao et al., 2008; Piccolo et al., 2013; Low et al., 2014).

Physical and functional interactions between TAZ and Thyroid Transcription Factor-1 (TTF-1, also named T-EBP/Nkx2.1) in the lung epithelial cells have raised the question of whether TAZ plays regulatory functions also in the thyroid (Park et al., 2004). The thyroid is one of the largest endocrine glands in mammals and is composed of two cone-like lobes or wings: *lobus dexter* (right lobe) and *lobus sinister* (left lobe) connected through the isthmus. Two types of cells are observed in the differentiated thyroid: the follicular cells producing thyroid hormones T3 (triiodothyronine) and T4 (thyroxine), and the parafollicular cells (also named C-cells) that secrete calcitonin (De Felice and Di Lauro, 2004). The thyroid follicular cell is characterized by the expression of thyroid differentiation markers: thyroglobulin (TG), sodium iodine symporter (NIS, Slc5a5), thyroperoxidase (TPO) and thyroid stimulating hormone (TSH) receptor (TSHR). To date, three transcription factors responsible for the expression of the thyroid differentiation markers have been identified: *TTF-1* (*Nkx2.1*, *nkx2.1a*), *Foxe1* and *Pax8* (Damante et al., 2001). These genes are coexpressed only in thyroid follicular cells. In particular, Pax8 seems to be the most important transcription factor for the differentiation and development of follicular cells; indeed its interaction with TTF-1 is needed to activate *Tg* transcription (Pasca di Magliano et al., 2000; Di Palma et al., 2003; Park et al., 2004). Pax8 and TTF-1 are part of a heterocomplex whose molecular mass is

greater than the sum of the two factors, suggesting the presence of other proteins. It has been demonstrated that TAZ is able to enhance the transcriptional activity of TTF-1 and Pax8 in immortalized thyroid cells. Furthermore, TAZ is able to support the activity exerted by TTF-1 and Pax8 on the *Tg* promoter (Di Palma et al., 2009).

In teleosts, the thyroid follicular tissue is loosely dispersed along the ventral midline of the pharyngeal mesenchyme and it is not encapsulated by connective tissue; in addition, thyroid follicular cells and C-cells are restricted to separate organs (Raine and Leatherland, 2000; Raine et al., 2001; Wendl et al., 2002). Despite species-specific variation in thyroid morphology and morphogenetic timing, transcription factors and molecular mechanisms involved in the induction and specification of the gland are conserved between mammals and zebrafish, with nkx2.1a/Nkx2.1 and pax2a/Pax8 acting presumably in the same manner (Wendl et al., 2002; Porazzi et al., 2009; Porreca et al., 2012). Therefore, zebrafish may well contribute to elucidating the molecular basis of thyroid development in higher vertebrates.

Although MO microinjection is a widely used approach in zebrafish, it is becoming increasingly clear that the resulting knockdown phenotype is not frequently observed in the corresponding mutant (Stainier et al., 2015). However, the effectiveness of the morpholino (MO)-based *wwtr1* down-regulation was previously assessed, by demonstrating the absence of the zebrafish Taz homolog in immunoblotting (Hong et al., 2005). It was reported that MO-mediated depletion of zebrafish Taz caused lack of ossification, cardiac edema and renal cysts (Hong et al., 2005; Tian et al., 2007). Histological studies of TAZ knockout mice showed cystic kidney but did not support a role in osteogenesis (Hossain et al., 2007). Further, the importance of TAZ-related YAP proteins in non-mammalian vertebrates has been revealed by studies in *Xenopus* and zebrafish, where Yap1 appears to regulate tissue growth and regeneration, and to be involved in endoderm formation, nephrogenesis and hair cell differentiation (Jiang et al., 2009; Skouloudaki et al., 2009; Gee et al., 2011; Hu et al., 2013; Hayashi et al., 2014; Loh et al., 2014; Fukui et al., 2015; He et al., 2015).

Herein, we have used zebrafish to study the role of Taz as a candidate regulator of thyroid development. The expression of the zebrafish *wwtr1* gene is detected in different domains of the embryo including the developing thyroid. Results from whole mount *in situ* hybridization (WISH), Real-time quantitative PCR (qPCR) and morphometric measurements of *wwtr1* knockdown phenotype indicate that zebrafish Taz is required for the correct size of the thyroid gland. In addition to previous studies showing that TAZ is a regulator of organ size (Pan et al., 2007) and that it promotes the proliferation of rat thyroid follicular FRTL-5 cells (De Cristofaro et al., 2011), this work results raise the possibility that TAZ has a central role in thyroid growth. Further, our studies

lend support to the concept that blood vessel morphogenesis is important for correct positioning of the thyroid follicles.

2. Results

2.1 Phylogeny and structure of zebrafish Taz.

Zebrafish *wwtr1* gene was previously recognized based on sequence alignment and similarity (Hong et al., 2005). The last assembly of the zebrafish genome (GRCz10), as released on September 2014 (GCA_000002035.3), indicated the presence of only one *wwtr1* gene homolog, suggesting that one copy of the gene was lost after the third round of whole genome duplication that occurred at the origin of the teleost clade (3R theory) (Amores et al., 1998) (Fig. 1). Interestingly, two *Wwtr1* paralogous genes were found in the dog genome as a result of gene duplication. Here, tree topology of TAZ evolution by Maximum Likelihood mirrored the traditional ordering of vertebrate classes (Fig. 1A). Likewise, phylogenetic relationships among YAP proteins, a subfamily of ancient TAZ orthologs of protostome origins, fit well with general assumptions on animal evolution (Fig. 1A). We next examined changes in sequence conservation among TAZ proteins using protein alignment by SIM (http://web.expasy.org/sim/) followed by graphical visualization by LalnView (Duret et al., 1996) (Fig. 1B). The evolutionary history of TAZ proteins showed deep sequence conservation (>50% identity) as seen in large regions of the zebrafish Taz protein. The percentage of TAZ protein identity was very high among mammals, in particular between *P. troglodytes* and *H. sapiens* (Fig. 1B).

2.2 Expression of wwtr1 in the thyroid primordium of zebrafish.

Murine *Wwtr1* is expressed in forebrain, hindbrain, somites and in the thyroid primordium during late stages of embryonic development (Di Palma et al., 2009). With the aim to investigate the expression profile of zebrafish *wwtr1*, WISH was performed using an antisense riboprobe against the full length mRNA. The fish *wwtr1* gene was expressed continuously from one-cell stage

through 4 days post fertilization (dpf). The message level was moderate and ubiquitously distributed until gastrula stage (Fig. 2A and B), then it increased in dorsal forebrain, hindbrain and adaxial cells (10-somite stage) (Fig. 2C-F). At 24 hours post fertilization (hpf), *wwtr1* mRNA was detected again across the entire embryo, with high level in brain, eyes, lateral line primordium and otic vesicles (Fig. 2G-J). From 42 hpf onwards, mRNA labeling was seen in lens, pharyngeal area, pectoral fin mesenchyme and in the thyroid primordium (Fig. 2K). At 48 hpf, a new signal appeared in the cephalic floor plate (Fig. 2L and M). Zebrafish *wwtr1* transcription in the thyroid was further supported by the observation of follicles immunoreactive for thyroglobulin in the pharyngeal domain of *wwtr1* expression (Fig. 2N). At 4 dpf, *wwtr1* expression is detected in brain, liver, gut, pectoral fins (stronger proximal), and cartilage elements of the craniofacial (branchial arches) and neurocranial (ethmoid plate and trabeculae) areas (Fig. 2O-S). At 4 dpf larval stage, *wwtr1* mRNA in the thyroid was no longer detectable by WISH (data not shown).

2.3 Development of the zebrafish thyroid without Taz.

Zebrafish embryos were injected at 1-2 cell stage with 1 ng of a MO against *wwtr1* AUG translational start site (Hong et al., 2005; Tian et al., 2007). Control embryos were injected with 1 ng of standard control-MO and found to be similar to uninjected embryos. Until 40 hpf, development of zebrafish *wwtr1* morphants was similar to that of control embryos. As previously shown, they later eventually developed heart edema typical of cardiovascular dysfunction, ventral trunk curvature and smaller head compared to controls (Hong et al., 2005). We examined the development of the thyroid gland in 48 hpf embryos by WISH experiments for thyroid transcription factors *nkx2.1a*, *pax2a* and *pax8*, and for thyroid differentiation genes *tg* and *scl5a5* (Rohr and Concha, 2000; Wendl et al., 2002; Elsalini et al., 2003). The abolition of Taz did not apparently alter the expression of the thyroid transcription factors and of the thyroid differentiation gene *scl5a5* in the thyroid primordium (Fig. 3A-F). Conversely, *tg* mRNA staining was stronger, likely due to the presence of more transcripts in the thyroid cells (Fig. 3G-J). qPCR analysis at 48 hpf partially confirmed WISH findings. Indeed, thyroid transcription factors *nkx2.1a* and *pax8* expression was not altered in *wwtr1* morphants. Conversely, *pax2a* expression was significantly reduced by qPCR, a finding not highlighted by WISH. This apparent divergence between WISH and qPCR results could be due to the wide domain of *pax2a* expression, making not easy to identify a 2-fold down-regulation of the transcript by WISH staining. Concerning thyroid differentiation genes, qPCR confirmed high *tg* expression shown by WISH in *wwtr1* knockdown embryos (Fig. 4). In particular, up-regulation of *scl5a5* likely reflected the ectopic expression seen in WISH experiments (Fig. 3I,J; Fig. 4). In addition, qPCR showed a significant up- and down-regulation of the *tpo* and *tshr* genes,

which were not analyzed by WISH (Fig. 4). Of note, *tshr*, *tg*, *tpo* and *slc5a5* expression is specific to zebrafish thyroid cells, while *nkx2.1a*, *pax2a* and *pax8* genes are also expressed in other embryonic tissues during zebrafish development.

2.4 Zebrafish Taz controls thyroid size.

Anti-TG and T4 antibodies immunochemistry was used to examine the maturation of thyroid follicles in *wwtr1*-MO embryos. Knockdown larvae showed no difference regarding labelling intensity in comparison to controls (Fig. 5). Follicles had successfully relocalized anteriorly into the pharyngeal tissue and were for the most part aligned along the midline (Fig. 5A,B). However, change in the location of thyroid follicles from midline was occasionally observed (Fig. 5C,D). Interestingly, the number of thyroid follicles was apparently reduced in larvae without Taz (Fig. 5A-F). One possible explanation is that Taz plays a role in regulating the number of thyroid follicles in zebrafish. We examined standard control-MO and *wwtr1*-MO injected larvae at 3 and 5 dpf. Follicle number ranged from 2 to 8 and from 0 to 6 in controls and morphants at 3 dpf, respectively, and from 2 to 9 and from 2 to 7 at 5 dpf, respectively. The median value was 53,8% greater in controls than in Taz-depleted larvae at 3 dpf ($p < 0.01$). At 5 dpf, difference in detectable follicles was less pronounced (26,2%) and not statistically supported ($p > 0.01$) (Tab. 1).

To find out whether the reduction in number is balanced by the expansion of individual follicles, we manually measured the raw diameter length of the lumen of 275 TG-positive thyroid follicles. At 3 dpf, the mean value was 30,1% greater in controls, ranging from 3,23 to 37,23 µm in controls and from 1,61 to 22,63 µm in morphants ($p < 0.01$), while at 5 dpf it ranged from 2,77 to 52,58 µm, and from 4,84 to 38,81 µm (11%; $p > 0.01$) (Tab. 1). Given that the thyroid of zebrafish consists of a long strand of loose follicles, a rough estimate of the mean lumen diameter of the thyroid gland follicles was calculated by multiplying the mean follicle number for the mean lumen diameter length. At 3 dpf, the lumen of the endocrine gland of larvae lacking Taz was 68,1% smaller than in control larvae, a difference that was reduced to 43,0% at 5 dpf (Tab. 1). Given that the Hippo pathway is implicated in controlling organ size by regulating cell number, immunohistochemistry (IHC) analyses were accompanied by counts of DAPI-positive *tg*-expressing cells in controls *vs wwtr1* morphants at 4 dpf (Fig. 6), documenting a statistically significant reduction (29,5%) of the mean number of follicular cells in thyroids (24,8) of morphant larvae compared to controls (35,2) ($p < 0,01$) (Tab. 1).

2.5 Taz depletion causes alteration of blood vessel patterning.

Following *wwtr1*-MO microinjection, a group of thyroid follicles (20,09%; n = 65) was found lateral to the ventral midline in 17,24 % morphant larvae at 4 dpf (Fig. 5D). It is known that late thyroid follicle localization in zebrafish is restricted to the midline area between the caudal aspect of the ceratohyal and the heart outflow tract (hypobranchial region), where follicles are physically associated to the endothelial cells of the ventral aorta and hypobranchial artery (Wendl et al., 2002; Alt et al., 2006a,b; Opitz et al., 2011, 2012). TAZ may be implicated in the formation of the circulatory system, as suggested by marked down-regulation in *Wwtr1*$^{-/-}$ mice of the *vascular endothelial growth factor receptor 2* (*vegfr2, kdr*) gene, a potential downstream target of TAZ protein (Mitani et al., 2009), and by evidence that the Hippo pathway mediates endothelial cell migration and angiogenesis (Dai et al., 2013). Therefore, we asked whether follicle positioning was influenced by *wwtr1* knockdown-specific vascular malformations. WISH and qPCR were used to analyze the transcriptional activity of the marker genes *tie-1* (Lyons et al., 1998) and *fli-1* (Brown et al., 2000) (Fig. 7A-F). Then, we examined the blood vessels of *wwtr1* knockdown embryos that carried the transgene tg(*kdr-like:gfp*), whose Green Fluorescent Protein expression is controlled by the promoter of the *kdr-like* gene and is used as a tool to monitor vascular architecture in the embryo (Jin et al., 2007) (Fig. 7G-I). At 48 hpf, spatial patterns (Fig. 7A-D) and quantitative levels (Fig. 7E,F) of gene expression were not significantly different between morphants and controls. Confocal microscopy study of 4 dpf tg(*kdr-like:gfp*) larvae that were labeled with T4 antibody revealed that vascular tree patterning was severely altered in the pharyngeal area of the *wwtr1* morphants, including loss of blood vessels or defects in connection, diameter and fusion (Fig. 7G-I). Some vessels were tentatively identifiable based on position and associations like in the case of opercular artery and first (branchial) aortic arch artery (Isogai et al., 2001). Another example is the ventral aorta, that failed to fuse into a midline channel in Taz-depleted larvae (Fig. 7G; Suppl. Video 1), where it still consisted of bilateral vessels (n = 14) (Fig. 7H,I; Suppl. Video 2). Interestingly, thyroid follicles were close to pharyngeal vessels but occasionally were not associated with ventral aorta (Fig. 7I).

Discussion

Until now, genetic work on the roles of the transcriptional co-activator TAZ, also referred as to Wwtr1, has revealed conserved and divergent traits in osteogenesis and nephrogenesis (Hong et al., 2005; Hossain et al., 2007; Tian et al., 2007). Our MO-mediated knockdown findings suggest that the zebrafish *wwtr1* gene is involved in thyroid size control, accounting for the reduced number

of thyroid follicles and thyroid follicle cells, and for the specific effect on the expression of thyroid differentiation genes. With the reported findings, we aim to provide new insights towards the understanding of the genetic mechanisms that regulate thyroid size.

3.1 Zebrafish Taz at the origin of vertebrate evolution

The gene encoding TAZ protein, *Wwtr1*, is found only in vertebrates, suggesting that its activity is associated with specific evolutionary innovations that evolved together with the taxonomic ordering of classes (Hilman and Gut, 2011). The origin of TAZ in vertebrates and the evolutionary events responsible for functional and structural specializations are still open questions. In various TAZ proteins along the phylogenetic scale of vertebrates, neo/subfunctionalization processes could be the result of the absence or presence of peculiar functional properties. Here, sequence alignment of vertebrate TAZ proteins shows that the major structural modifications occurred during the fish-tetrapod transition. The importance of TAZ and in general of the Hippo pathway in zebrafish development is emphasized by expression data that point at the interaction between Taz and Yap1 in several morphological domains, likely including the thyroid gland (Fig. 2) (Jiang et al., 2009; this work).

3.2 Taz and thyroid gland size

TAZ and its paralog YAP are part of the Hippo pathway, known to be responsible of a universal organ size-mechanism, under the influence of developmental cues such as cell density (Dong et al., 2007; Kango-Singh and Singh, 2009). It has been recently proposed that TAZ plays a central role in conveying biomechanical properties associated to tissue growth and organ size at the cellular level (Halder et al., 2012). A genetic screen for tumor suppressor genes in *Drosophila* allowed identifying the Hippo signaling pathway, an evolutionarily conserved mechanism that controls organ size by sensing mechanical and cytoskeletal signals associated to cell density (Edgar, 2006). The core components of the Hippo-YAP pathway are two kinases, Lts and Wts, which inactivate the downstream effector Yorkie through direct phosphorylation. The Yes-associated protein (YAP) and TAZ are the vertebrate homologs of Yorkie. Following phosphorylation, TAZ is retained in the cytoplasm where it interacts with TEA domain (TEAD) transcription factors. There is gathering evidence that the Hippo pathway controls cell number by repressing cell proliferation and inducing apoptosis of non-stem/progenitor cells and promotes cell proliferation and self-renewal of stem/progenitor cells, a function that is mediated by the interaction with TGFβ signaling (Zhao et al., 2007, 2010; Lei et al., 2008; Varelas et al., 2008, 2010; Dupont et al., 2011). In turn, the Hippo pathway is regulated by extracellular factors as well as mechanical stimuli that influence

the actin cytoskeleton (Dupont et al., 2011; Calvo et al., 2013; Low et al., 2014; Matsui and Lai, 2014; Varelas, 2014).

It was previously shown *in vitro* that TAZ forms a heterocomplex with Pax8 and TTF-1 to exert its function as a transcriptional modulator of these two transcription factors, and that such interaction brings to a strong activation of the *Tg* gene promoter (Di Palma et al., 2009). It is not yet known, however, whether the same condition pertains *in vivo*. Compared with amphibians and mammals, the expression pattern of the zebrafish *wwtr1* orthologue has conserved (brain, head cartilage and somites) and distinct (paired appendages) domains (Nejigane et al., 2011; Di Palma et al., 2009). Like in mouse, zebrafish *wwtr1* starts to be expressed during the re-localization phase of the thyroid primordium (Fig. 2K). Our study strongly suggests that zebrafish plays a role in thyroid gland differentiation. By means of WISH and qPCR, we found that *wwtr1* knockdown significantly affects the expression of thyroid differentiation genes, including some whose mammalian orthologues were not previously studied with respect to the transcriptional coactivator TAZ (Di Palma et al., 2009). The observed up-regulation of *tg* is in contrast with data in a mammalian *in vitro* system (Di Palma et al., 2009). The difference on the effect of TAZ loss on *Tg* expression suggests different functions in thyroid development. This is not surprising based on recent observation of Crumbs protein signalling effect on Hippo pathway between *Drosophila* and mammalian cells (Miesfeld et al., 2014). However, we should still consider the molecular (*i.e.*, the functional role of *pax2a* instead of *pax8*) and anatomical (*i.e.*, thyroid follicle tissue encapsulated or loosely dispersed; thyroid follicular cells and C-cells in same or separate organs) differences observed between mammalian and zebrafish thyroid (Raine and Leatherland, 2000; Raine et al., 2001; Wendl et al., 2002).

A reduction in number of thyroid follicles and thyroid follicle cells that are able to differentiate and produce hormones in the thyroid gland was detected in *wwtr1*-MO injected larvae (Tab. 1). In line with the role of TSH and TSHR in proliferation of thyroid cells (Dumont et al., 1992; Vassart and Dumont, 1992; Opitz et al., 2011), *tshr* expression is significantly reduced in *wwtr1* morphants, suggesting that changes in the expression of thyroid differentiation genes may be detrimental to gland maturation (Fig. 4). That TAZ expression confers growth advantage in rat thyroid follicular FRTL-5 cells and is up-regulated in papillary thyroid carcinoma reinforces the suggestion that this transcriptional coactivator is involved in thyroid growth control (De Cristofaro et al., 2011). It will be interesting to analyze the role of TAZ with respect to congenital hypothyroidism in humans. Notably, TAZ is not a frequent cause of thyroid dysgenesis. No germline mutations of *WWTR1* have been detected in about 100 patients affected by this congenital deficiency, suggesting that TAZ has an essential role in embryonic development (Ferrara et al.,

2009). It remains unclear whether TAZ function in thyroid growth is exerted by regulating cellular processes of proliferation, apoptosis or both. Finally, partial recovery of thyroid gland size in *wwtr1* MO larvae is not perhaps surprising since there appears to be significant redundancy in the Hippo pathways. It also suggests that the decrease in thyroid size in *wwtr1* knockdown zebrafish is not linked to the observed deformation of the hypobranchial region (the space available for thyroid follicles to populate) likely caused by cartilage loss and heart edema (Hong et al., 2005; Tian et al., 2007; Wang et al., 2009; Hong and Guan, 2012).

3.3 Abnormal blood vessel morphology correlates with thyroid follicle displacement.

In zebrafish *wwtr1* morphants, thyroid follicles may occasionally escape midline alignment towards dorsal and lateral positions, challenging the essential role of the ventral aorta in terminal re-localization (Fig. 5C-F). The dependence of thyroid morphogenesis on the development of adjacent arteries is a conserved mechanism that might have evolved to ensure efficient hormone release into circulation (Alt et al., 2006b; Fagman et al., 2004, 2006; Opitz et al., 2011, 2012). In zebrafish, Taz-deprived embryos showed severe morphological and growth anomalies of pharyngeal blood vessels, with loss of (branchial) aortic arch arteries (Fig. 7G-I). The vascular pattern could be affected by the absence of cartilages and bones, suggesting that TAZ function, as molecular "rheostat" in osteogenesis, is relevant for proper positioning of thyroid follicles (Hong et al., 2005). However, that TAZ plays specific functions in blood vessel morphogenesis should be investigated. Fusion plays a major role in vessel remodeling, and is regulated by the interplay of several promoting and inhibiting factors. TGFß signaling performs both roles (Oh et al., 2000; Garriock et al., 2010) but it generally suppresses proliferation and migration depending on the presence of other factors, such as VEGF (Drake and Little, 1999; Holderfield and Hughes, 2008). Due to the role of TAZ in promoting SMAD2/3/4 accumulation in the nucleus (Varelas et al., 2008), it is worth suggesting that the zebrafish orthologous protein, Taz, exerts a role in blood vessel fusion through direct regulation of TGFß signaling downstream factors. An *in vivo* view of blood vessel development will help in addressing possible implication of Taz in ventral aorta fusion. Likewise, it is plausible that *wwtr1* is not expressed in blood vessels and thereby it is not required for vessel remodeling. In future, rescue of blood vessel patterning in *wwtr1* morphants may help to show if Taz regulates thyroid follicle position via blood vessel patterning. Consistent with previous studies (Alt et al., 2006a,b; Opitz et al., 2011, 2012), terminal localization of thyroidal follicles in zebrafish depends on proper vascular architecture. That thyroid follicles are invariably associated to blood vessels reinforces the idea that the circulatory system provides a fundamental guide for thyroid follicle positioning.

Experimental Procedures

4.1 Zebrafish

Zebrafish work was carried out according to standard procedures (Westerfield, 2000) and in accordance with European Union animal welfare guidelines. Staging in hours post fertilization (hpf) or days post fertilization (dpf) refers to development at 28.5 °C. We used the transgenic fish line tg(*kdr-like:gfp*) (Habeck et al., 2002).

4.2 Embryonic manipulation

An antisense morpholino oligonucleotide directed against the zebrafish Taz translation initiation codon (*wwtr1*-MO: 5'-CTGGAGAGGATTACCGCTCATGGTC-3') was purchased from GeneTools LLC. Zebrafish embryos at 1-cell stage were injected with 1 ng of *wwtr1*-MO in 1 × Danieau buffer (58 mM NaCl, 0.7 mM KCl, 0.4 mM $MgSO_4$, 0.6 mM $Ca(NO_3)_2$, 5 mM Hepes pH 7.6). All phenotypes described were found in more than 70% morphants, with the rest showing milder defects or wild-type appearance. Effects of *wwtr1*-MO injection were determined by including uninjected or standard control-MO (5'-CCTCTTACCTCAGTTACAATTTATA-3') injected wild-type zebrafish in the analysis. Both control groups exhibited similar morphology and gene expression, reported findings were therefore chosen from both groups based on image quality.

Phylogenetic analysis

To find orthologs of TAZ and YAP, we employed BLAST analysis of zebrafish Taz and Yap1 sequences against the genome of several species using both ENSEMBL and NCBI databases and only sequences with high blast score were considered. Sequence alignments were performed on orthologous proteins using MUSCLE (Edgar, 2004) with default parameters. Phylogenetic analysis was conducted using PhyML (Guindon and Gascuel, 2003; Guindon et al., 2005) and FastTree (Price et al., 2010) for Maximum likelihood (ML) analysis, with default parameters. Neighbor joining (NJ) trees were built using MEGA5 (Kumar et al., 2008) (data not shown). Pair-wise alignment of TAZ protein sequences was performed with SIM (http://web.expasy.org/sim/) and graphically visualized by LalnView (http://pbil.univ-lyon1.fr/software/lalnview.html) (Duret et al., 1996).

4.4 Whole mount in situ hybridization, immunohistochemistry and histology

Zebrafish *wwtr1* full length cDNA was cloned into pCR II-TOPO vector (Invitrogen, Carlsbad, CA). Experiments were performed according to Thisse and colleagues (Thisse et al., 1993) using antisense digoxygenin-labeled riboprobes and BM Purple (Roche) as staining substrate, or the antisense fluorescein-labeled riboprobe for *tg* mRNA and FastRed (Roche) as staining substrate. For immunostaining, 4-5 dpf paraformaldehyde-fixed embryos were labeled with polyclonal anti-thyroglobulin antibody (1:6000 rabbit anti-human thyroglobulin, Dako), polyclonal anti-T4 antibody (1:4000, MP Biochemicals) and monoclonal anti-GFP antibody A11120 (1:250, Invitrogen) as previously described (Elsalini et al., 2003). Stained specimens were dehydrated in 70% EtOH, embedded in Epon resin, and sectioned for histology. To determine cell numbers, sample labeled for immunohistochemistry were incubated with DAPI (1:10000, Sigma) in PBT and incubated overnight at 4 °C.

4.5 Microscopy

Embryos processed for WISH and immunohistochemistry were bleached, mounted in 80% glycerol and imaged using an AxioPlan 2 and an AxioImager microscope equipped with Axiocam digital camera (Zeiss). Images were processed using Axio Vision software. For fluorescent images, embryos were mounted in 0.5% Agarose and then examined and photographed using Leica SPE confocal microscope. Images were processed using Leica LASAF lite software. 3D reconstructions were generated with Volocity (Perkin Elmer) imaging analysis software.

4.6 Morphometric analysis

There is no mathematical transformation able to convert data obtained by conventional microscopy of whole mount zebrafish into true sizes of follicles. Follicles vary in size, with most bodies being spherical in shape. The main follicle axis is therefore considered as length of follicle raw diameter. The method overestimated elongated follicles, but comparisons were still possible because of the large number of measurements (Faggiano et al., 2004). Here, we counted a total of 297 thyroid follicles and measured the main follicle axis of 275 of them by AxioImager (Zeiss) compound microscope. For thyroid follicle cell counting, 4 dpf larvae injected with standard control-MO and *wwtr1*-MO (4 dpf, 10/10) were co-labeled with DAPI and *tg* riboprobe, and then analyzed by confocal microscopy (LSM 510 META, Zeiss). Then, a single observer performed manual counting of thyroid follicle cell nuclei in confocal z-stack images using ImageJ. The statistical significance of differences was determined using Student's unpaired *t* test and was set at $p < 0.01$.

4.7 Real-time quantitative PCR

Total RNA was isolated from zebrafish embryos using Trizol reagent (Invitrogen) following manufacturer's instructions. RNA concentration and integrity were estimated using a NanoDrop ND-1000 spectrophotometer and by gel electrophoresis, respectively. First-strand cDNA was synthesized from 2 µg total RNA using the QuantiTect Rev. Transcription Kit (Qiagen) according to manufacturer's instructions. qPCR was conducted using a 7009 HT Analyzer and SYBR Green Chemistry (Applied Biosystems). Thermal cycling parameters were 95°C for 30 s, 60°C for 1 min, 40 cycles, followed by a denaturation step to verify the presence of a single amplification product. Specific primer pairs for each gene analyzed are listed below: *tg* forward 5'-CCAGCCGAAAGGATAGAGTTG-3' and reverse 5'-ATGCTGCCGTGGAATAGGA-3'; *tshr* forward 5'- CTCCTTGATGTGTCCGAAT-3' and reverse 5'-CGGGCAGTCAGGTTACAAAT-3'; *tpo* forward 5'- CCAACTTCCTCCGGTTCGAG-3' and reverse 5'-AAGCAGGGATCTGCACTGAC-3'; *slc5a5* forward 5'-GGTGGCATGAAGGCTGTAAT-3' and reverse 5'-GCCTGATTGGCTCCATACAT-3'; *nkx2.1a* forward 5'-GGTGCAATGGGGGACCTGCC-3' and reverse 5'-CCTGGAGATTGTTGGGTATCTCGGC-3'; *pax8* forward 5'-GAAGATCGCGGAGTACAAGC-3' and reverse 5'-CTGCACTTTAGTGCGGATGA-3'; *pax2a* forward 5'-CCGCGTTATTAAGTTCCCCT-3' and reverse 5'-TGGCGTATCCATCTTCAATCC-3'; *rpl13a* forward 5'-TCTGGAGGACTGTAAGAGGTATGC-3' and reverse 5'-AGACGCACAATCTTGAGAGCAG-3'; *ßactin* forward 5'-TCTCTTAAGTCGACAACCCCC-3' and reverse 5'-TCTGAGCCTCATCACCAACG-3'; *elfa1* forward 5'-ACCTACCCTCCTCTTGGTCG -3', reverse 5'-GGAACGGTGTGATTGAGGGA-3'. Result analysis was performed following real-time relative quantitation guidelines through the relative standard curve method as suggested by Applied Biosystems. Briefly, the amplification efficiency of each primer pair was calculated from triplicate relative standard curves for each primer pair using the equation $E = 10^{-1/slope}$ and then used to convert Ct values obtained from each reaction into relative-expression units. Data obtained in this way were then normalized on the relative expression of three reference genes, *rpl13a, elfa1* and *ßactin* which are known to be expressed at constant levels during the first 72 hpf (McCurley and Callard, 2008; Tang et al., 2007). qPCR data were normalized with the aforesaid reference genes by calculating the geometric mean of the expression of the different reference genes in order to normalize gene transcription levels (Vandesompele et al., 2002). qPCR experiments were performed three times on three independent pools of control and *wwtr1*-MO injected embryos (50 embryos per pool). Data are reported as mean value of the three experiments. The statistical

significance of differences on the three experiments was determined using Student's unpaired *t* test and was set at $p < 0.01$.

Acknowledgments

The authors thank anonymous reviewers for constructive comments on earlier versions of this paper, R. Boni for statistical analysis, Electron Microscopy Service at SZN for technical help, M. Ferrante and M. Santoro for critical reading of the manuscript, and members of the groups for discussions. In particular, we wish to thank A. E. Fortunato, E. Van Rooijen and F. Langellotto for valuable suggestions and assistance. This research was supported by Italian Ministry of Education and Research (MIUR) grants "MouZe Clinic" PONa3_00239 to E.D.F., "Progetti Premiali 2011" to L.C., and FIRB (RBFR12QW4I) to P.S.

References

Alt, B., et al., 2006a. Arteries define the position of the thyroid gland during its developmental relocalisation. Development 133, 3797–3804.

Alt, B., et al., 2006b. Analysis of origin and growth of the thyroid gland in zebrafish. Dev. Dyn. 235, 1872–1883.

Brown, L.A., et al., 2000. Insights into early vasculogenesis revealed by expression of the ETS-domain transcription factor Fli-1 in wild-type and mutant zebrafish embryos. Mech. Dev. 90, 237–252.

Calvo, F., et al., 2013. Mechanotransduction and YAP- dependent matrix remodelling is required for the generation and maintenance of cancer-associated fibroblasts. Nat. Cell Biol. 15, 637–646

Dai, X., et al., 2013. Phosphorylation of angiomotin by Lats1/2 kinases inhibits F-actin binding, cell migration, and angiogenesis. J. Biol. Chem. 288, 34041–43051.

Damante, G., et al., 2001. A unique combination of transcription factors controls differentiation of thyroid cells. Prog. Nucleic Acid Res. Mol. Biol. 66, 307–356.

De Cristofaro, T., et al., 2011. TAZ/WWTR1 is overexpressed in papillary thyroid carcinoma. Eur. J. Cancer 47, 926–933.

De Felice, M., Di Lauro, R., 2004. Thyroid development and its disorders: genetics and molecular mechanisms. Endocrine Rev. 25, 722–746.

Di Palma, T., et al., 2003. The paired domain-containing factor Pax8 and the homeodomain-containing factor TTF-1 directly interact and synergistically activate transcription. J. Biol. Chem. 278, 3395–3402.

Di Palma, T., et al., 2009. TAZ is a coactivator for Pax8 and TTF-1, two transcription factors involved in thyroid differentiation. Exp. Cell Res. 315, 162–175.

Dong, J., et al., 2007. Elucidation of a universal size-control mechanism in *Drosophila* and mammals. Cell 130, 1120–1133.

Drake, C.J., Little, C.D., 1999. VEGF and vascular fusion: Implications for normal and pathological vessels. J. Histochem. Cytochem. 47, 1351–1355.

Dumont, J.E., et al., 1992, Physiological and pathological regulation of thyroid cell proliferation and differentiation by thyrotropin and other factors. Physiol. Rev. 72, 667–697.

Dupont, S., et al. 2011. Role of YAP/TAZ in mechanotransduction. Nature 474:179–183

Duret L., Gasteiger E., Perriere G., 1996, LalnView: a graphical viewer for pairwise sequence alignments. Comput. Applic. Biosci. 12, 507–510.

Edgar, B.A., 2006. From cell structure to transcription: Hippo forges a new path. Cell 124, 267–273.

Edgar, R.C., 2004. MUSCLE: multiple sequence alignment with high accuracy and high throughput. Nucleic Acids Res. 32, 1792–1797.

Elsalini, O.A., et al., 2003. Zebrafish hhex, nk2.1a, and pax2a regulate thyroid growth and differentiation downstream of Nodal-dependent transcription factors. Dev. Biol. 263, 67–80.

Faggiano, A., et al., 2004. Age-dependent variation of follicular size and expression of iodine transporters in human thyroid tissue. J. Nucl. Med. 45, 232–237.

Fagman, H., et al., 2004. Genetic deletion of *Sonic hedgehog* causes hemiagenesis and ectopic development of the thyroid in mouse. Am. J. Pathol. 164, 1865–1872.

Fagman, H., et al., 2006. The developing mouse thyroid: embryonic vessel contacts and parenchymal growth pattern during specification, budding, migration, and lobulation. Dev. Dyn. 235, 444–455.

Fagman, H. et al., 2011. Gene expression profiling at early organogenesis reveals both common and diverse mechanisms in foregut patterning. Dev. Biol. 359, 163–175.

Ferrara, A.M., et al., 2009. Mutations in TAZ/WWTR1, a co-activator of NKX2.1 and PAX8 are not a frequent cause of thyroid dysgenesis. J. Endocrinol. Invest. 32, 238–241.

Fukui, H., 2015. S1P-Yap1 signaling regulates endoderm formation required for cardiac precursor cell migration in zebrafish. Dev. Cell 31, 128–136.

Garriock, R.J., et al., 2010. An anteroposterior wave of vascular inhibitor downregulation signals aortae fusion along the embryonic midline axis. Development 137, 3697–3706.

Gee, S.T., et al., 2011. Yes-Associated Protein 65 (YAP) expands neural progenitors and regulates Pax3 expression in the neural plate border zone. PLoS ONE 6, e20309.

Guindon, S., Gascuel, O., 2003. A simple, fast, and accurate algorithm to estimate large phylogenies by maximum likelihood. Syst Biol. 52, 696–704.

Guindon, S., et al., 2005. PHYML online—a web server for fast maximum likelihood-based phylogenetic inference. Nucleic Acids Res. 33, W557–W559.

Habeck, H., et al., Tübingen 2000 screen consortium, 2002. Analysis of a zebrafish VEGF receptor mutant reveals specific disruption of angiogenesis. Curr. Biol. 12, 1405–1412.

Halder, G., Dupont, S., Piccolo, S., 2012. Transduction of mechanical and cytoskeletal cues by YAP and TAZ. Nature Rev. Mol. Cell Biol. 13, 591–600.

Hayashi, S., Tamura, K., Yokoyama, H., 2014. Yap1, transcription regulator in the Hippo signaling pathway, is required for *Xenopus* limb bud regeneration. Dev. Biol. 388, 57–67.

He, L., et al., 2015. Yes-Associated Protein (Yap) is necessary for ciliogenesis and morphogenesis during pronephros development in zebrafish (*Danio rerio*). Int. J. Biol. Sci. 11, 935–947.

Hilman, D., Gat, U., 2011. The evolutionary history of YAP and the Hippo/YAP pathway. Mol. Biol. Evol. 28, 2403–2417.

Holderfield, M.T., Hughes, C.C., 2008. Crosstalk between vascular endothelial growth factor, notch, and transforming growth factor-beta in vascular morphogenesis. Circ. Res. 102, 637–652.

Hong, J.H., et al., 2005. TAZ, a transcriptional modulator of mesenchymal stem cell differentiation. Science 309, 1074–1078.

Hong, W., Guan, K.L., 2012. The YAP and TAZ transcription coactivators: key downstream effectors of the mammalian Hippo pathway. Semin. Cell Dev. Biol. 23, 785–793.

Hossain, Z., et al., 2007. Glomerulocystic kidney disease in mice with a targeted inactivation of Wwtr1. Proc. Natl. Acad. Sci. USA 104, 1631–1636.

Hu, J., et al., 2013. Yes-associated protein (Yap) is required for early embryonic development in zebrafish (*Danio rerio*). Int. J. Biol. Sci. 9, 267–278.

Isogai, S., et al., 2001. The vascular anatomy of the developing zebrafish: an atlas of embryonic and early larval development. Dev. Biol. 230, 278–301.

Jiang, Q., et al., 2009. *yap* is required for the development of brain, eyes, and neural crest in zebrafish. Biochem. Biophys. Res. Commun. 384, 114–119.

Jin, S. W., et al., 2007. A transgene assisted genetic screen identifies essential regulators of vascular development in vertebrate embryos. Dev. Biol. 307, 29–42.

Kanai, F., et al., 2000. TAZ: a novel transcriptional co-activator regulated by interactions with 14-3-3 and PDZ domain proteins. EMBO J. 19, 6778–6791.

Kango-Singh, M., Singh, A., 2009. Regulation of organ size: insights from the *Drosophila* Hippo signaling pathway. Dev. Dyn. 238, 1627–1637.

Kodaka, M., Hata, Y., 2015. The mammalian Hippo pathway: regulation and function of YAP1 and TAZ. Cell. Mol. Life Sci. 72, 285-306.

Kumar, S., et al., 2008. MEGA: a biologist-centric software for evolutionary analysis of DNA and protein sequences. Brief Bioinform. 9, 299–306.

Lei, Q.Y., et al., 2008. TAZ promotes cell proliferation and epithelial-mesenchymal transition and is inhibited by the Hippo pathway. Mol. Cell. Biol. 28, 2426–2436.

Loh, S.-L., et al., 2014. Zebrafish *yap1* plays a role in differentiation of hair cells in posterior lateral line. Sci. Rep. 4, 4289.

Low, B.C., et al., 2014. YAP/TAZ as mechanosensors and mechanotransducers in regulating organ size and tumor growth. FEBS Let. 588, 2663–2670.

Lyons, M.S., et al., 1998. Isolation of the zebrafish homologues for the tie-1 and tie-2 endothelium-specific receptor tyrosine kinases. Dev. Dyn. 212, 133–140.

Matsui, Y., Lai, Z.C., 2014. Mutual regulation between Hippo signaling and actin cytoskeleton Protein Cell 4, 904–910.

McCurley, A.T., Callard, G.V., 2008. Characterization of housekeeping genes in zebrafish: male-female differences and effects of tissue type, developmental stage and chemical treatment. BMC Mol. Biol. 9, 102.

Miesfeld, J.B., Link, B.A., 2014. Establishment of transgenic lines to monitor and manipulate Yap/Taz-Tead activity in zebrafish reveals both evolutionarily conserved and divergent functions of the Hippo pathway. Mech. Dev. 133, 177-188.

Mitani, A., et al., 2009. Transcriptional coactivator with PDZ-binding motif is essential for normal alveolarization in mice. Am. J. Resp. Critical Care Med. 180, 326–338.

Nejigane, S., et al., 2011. The transcriptional coactivators Yap and TAZ are expressed during early *Xenopus* development. Int. J. Dev. Biol. 55, 121-126.

Oh, S.P., et al., 2000. Activin receptor-like kinase 1 modulates transforming growth factor-β1 signaling in the regulation of angiogenesis. Proc. Natl. Acad. Sci. USA 97, 2626–2631.

Opitz, R., et al., 2011. TSH receptor function is required for normal thyroid differentiation in zebrafish. Mol. Endocrinol. 25, 1579–1599.

Opitz, R., et al., 2012. Transgenic zebrafish illuminate the dynamics of thyroid morphogenesis and its relationship to cardiovascular development. Dev. Biol. 372, 203–216.

Pan, D., 2007. Hippo signaling in organ size control. Genes Dev. 21, 886–897.

Park, K-S., et al., 2004. TAZ interacts with TTF-1 and regulates expression of Sulfactant Protein-C. J. Biol. Chem. 279, 17384–17390.

Pasca di Magliano, M., et al., 2000. Pax8 has a key role in thyroid cell differentiation. Proc. Natl. Acad. Sci. USA 97, 13144–13149.

Piccolo, S., Cordenonsi, M., Dupont, S., 2013. Molecular pathways: YAP and TAZ take center stage in organ growth and tumorigenesis. Clin. Cancer Res. 19, 4925–4930.

Piccolo, S., Dupont, S., Cordenonsi, M., 2014. The biology of YAP/TAZ: Hippo signaling and beyond. Physiol. Rev. 94, 1287–1312.

Porazzi, P., et al., 2009. Thyroid gland development and function in the zebrafish model. Mol. Cell. Endocrinol. 312, 14–23.

Porreca, I., et al., 2012. Zebrafish *bcl2l* is a survival factor in thyroid development. Dev. Biol. 366, 142–152.

Price, M.N., et al., 2010. FastTree 2—approximately maximum-likelihood trees for large alignments. PloS One 5, e9490.

Raine, J.C., Leatherland J.F., 2000. Morphological and functional development of the thyroid tissue in rainbow trout (*Oncorhynchus mykiss*) embryos. Cell Tissue Res. 301, 235–244.

Raine, J.C., et al., 2001. Assessment of thyroid function in adult medaka (*Oryzias latipes*) and juvenile rainbow trout (*Oncorhynchus mykiss*) using immunostaining methods. J. Exp. Zool. 290, 366–378.

Rohr, K.B., Concha, M.L., 2000. Expression of *nk2.1a* during early development of the thyroid gland in zebrafish. Mech. Dev. 95, 267–270.

Rutledge, R.G., Cote, C., 2003. Mathematics of quantitative kinetic PCR and the application of standard curves. Nucleic Acids Res. 31, e93.

Saucedo, L.J., Edgar, B.A., 2007. Filling out the Hippo pathway. Nat. Rev. Mol. Cell Biol. 8, 613–621.

Stainier, D.Y.R., et al., 2015. Making sense of anti-sense data. Dev. Cell 32, 7–8.

Skouloudaki, K., et al., 2009. Scribble participates in Hippo signaling and is required for normal zebrafish pronephros development. Proc. Natl. Acad. Sci. USA 106, 8579–8584.

Tang, R., et al., 2007. Validation of zebrafish (*Danio rerio*) reference genes for quantitative real-time RT-PCR normalization. Acta Biochim. Biophys. Sin. (Shanghai) 39, 384–390.

Thisse, C., et al., 1993. Structure of the zebrafish *snail1* gene and its expression in wild-type, spadetail and no tail mutant embryos. Development 119, 1203–1215.

Tian, Y., et al., 2007. TAZ promotes PC2 degradation through a SCFbeta-Trcp E3 ligase complex. Mol. Cell. Biol. 27, 6383–6395.

Vandesompele, J., et al., 2002. Accurate normalization of real-time quantitative RT-PCR data by geometric averaging of multiple internal control genes. Genome Biol. 3: research0034-research0034.11.

Varelas, X., et al., 2008. TAZ controls Smad nucleocytoplasmic shuttling and regulates human embryonic stem-cell self-renewal. Nat. Cell Biol. 10, 837–848.

Varelas, X., et al., 2010. The Crumbs complex couples cell density sensing to Hippo-dependent control of the TGF-β-SMAD pathway. Dev. Cell 19, 831–844.

Varelas, X., 2014. The Hippo pathway effectors TAZ and YAP in development, homeostasis and disease. Development 141, 1614–1626.

Vassart, G., Dumont, J.E., 1992. The thyrotropin receptor and the regulation of thyrocyte function and growth. Endocr. Rev. 13, 596–611.

Wang, K, et al., 2009. YAP, TAZ, and Yorkie: a conserved family of signal-responsive transcriptional coregulators in animal development and human disease. Biochem. Cell. Biol. 87, 77–91.

Wendl, T., et al., 2002. *pax2.1* is required for the development of thyroid follicles in zebrafish. Development 129, 3751–3760.

Westerfield, M.**,** 2000. The zebrafish book: a guide for the laboratory use of zebrafish (*Danio rerio*). University of Oregon, Eugene.

Zhao, B., et al., 2007. Inactivation of YAP oncoprotein by the Hippo pathway is involved in cell contact inhibition and tissue growth control. Genes Dev. 21, 2747–2761.

Zhao, B., Lei, Q.Y., Guan, K.L., 2008. The Hippo-YAP pathway: new connections between regulation of organ size and cancer. Curr. Opin. Cell Biol. 20, 638–646.

Zhao, B., et al., 2010. The Hippo-YAP pathway in organ size control and tumorigenesis: an updated version. Genes Dev. 24, 862–874.

Figure legends

Figure 1. High evolutionary conservation of TAZ transcriptional coactivators. Tree topology by Maximum Likelihood is consistent with general assumptions on vertebrate taxonomy (A). Schematic alignment of TAZ proteins (B).

Figure 2. Zebrafish *wwtr1* mRNA expression. WISH data from 8-cell stage to 96 hpf. *Wwtr1* mRNA is maternally provided (A) and then ubiquitously distributed at low levels during gastrulation (B) and early somitogenesis (C), when a strong signal is detected in dorsal forebrain (D), hindbrain (E) and adaxial cells (F). Diffuse expression at 24 hpf, with strong expression in brain (G), eye (lens and retina) (H), otic vesicles (I) and lateral line primordium (J). At 42 and 48 hpf, *wwtr1* mRNA is seen in lens, pectoral fins and pharyngeal area (K-N). Transverse section of a 60 hpf embryo showing a large domain of *wwtr1 mRNA*-positive cells covering the pharyngeal tissue and the thyroid follicle with TG immunostaining depicted (N). At 96 hpf, *wwtr1* is expressed in pectoral fins (P), liver and gut (Q), anterior craniofacial (R) and neurocranial (S) cartilages. Arrowheads indicate higher level of expression in the pectoral fin mesenchyme proximally (O and P) Scale bar = 200 µm. 3-7, (branchial) aortic arch arteries; df, dorsal forebrain, ac, adaxial cells; cp, cephalic floor plate; di, diencephalon; ep, ethmoid plate; ey, eye; fm, fin mesenchyme; ff, fin fold; gt, gut; hb, hindbrain; le, lens; l, liver; lp, lateral line primordium; m, mouth; mb, midbrain-hindbrain boundary; n, notochord; ov, otic vesicle; pc, polar cartilage; pf, pectoral fin; ph, pharyngeal tissue; te, telencephalon; tl, thyroid follicle lumen; tf, thyroid follicular cells; tp, thyroid primordium; tr, trabeculae. Anterior is to the left in dorsal (A, D-F), ventral (R and S) and lateral view (B, C, G-L, Q). In (M), anterior is to the top in dorsal view.

Figure 3. *wwtr1*-MO injection effect on the expression of thyroid transcription factors and thyroid specific genes. 48 hpf zebrafish embryos uninjected (uninj) (A and C) and injected with standard control-MO (scMO) (E, G, I) and *wwtr1*-MO (B, D, F, H, J), hybridized with probes for thyroid transcription factors *nkx2.1a*, *pax2a* and *pax8*, and thyroid differentiation genes *tg* and *slc5a5* (A-H). Arrowheads indicate the thyroid gland. Asterisk depicts specific *nkx2.1a* mRNA signal over high staining background (B). Scale bar = 200 µm. Anterior is to the left in lateral view.

Figure 4. Real-time quantitative PCR. Injected with standard control-MO (dark grey) and *wwtr1*-MO (light grey). Expression fold change of the *tshr*, *tpo*, *tg*, *slc5a5*, *nkx2.1a*, *pax2a* and *pax8* genes

relative to *rpl13a*, *ß-actin* and *elfa1* (G) and based on qPCR. The results are the average of three independent experiments conducted on pools of 50 embryos each (** $p < 0.01$).

Figure 5. Whole-mount immunostaining of T4 and TG. Uninjected (Uninj) (A), injected with standard control-MO (scMO) (C and E) and *wwtr1*-MO (B, D, F) 4 dpf larvae were immunolabeled for T4 (A-D) and TG (E and F). Thyroid follicles are reduced in number (A-D) and not restricted to the ventral midline in Taz-deprived larvae (C-F). Arrowheads indicate thyroid follicles. Scale bar represents 200 µm (A, B, E, F) and 100 µm (C and D). Anterior is to the left in ventral (A-D) and lateral views (E and F).

Figure 6. Zebrafish Taz controls the number of thyroid follicular cells. Z-stack images of *tg* mRNA labeling in DAPI stained zebrafish at 4 dpf injected with standard control-MO (A) and *wwtr1*-MO (B). Arrows indicate nuclei of *tg* expressing thyroid follicle cells. Scale bar represents 100 µm.

Figure 7. *wwtr1*-MO injection effect on endothelial marker expression and vascular tree morphology. WISH analysis with riboprobes against *fli-1* and *tie-1* mRNA at 48 hpf (A-D), and qPCR analysis where fold change is relative to *rpl13a* (E and F), show comparable results in uninjected (A and C) and standard control-MO (scMO) zebrafish (48 hpf). qPCR results are the average of two independent experiments conducted on pools of 50 embryos each ($p > 0.01$). Zebrafish injected with standard control-MO (dark grey) and *wwtr1*-MO (light grey), H, I). Scale bar = 200 µm. Anterior is to the left in lateral view. (G-I) Vasculature of *wwtr1* morphant larvae is altered in the pharyngeal region of tg(*kdr-like:gfp*) zebrafish (4 dpf), with patterning defects and loss of blood vessels. Pharyngeal vessels and thyroid follicles were immunolabeled for GFP (green) and T4 antibody (red) in 4 dpf larvae. Uninjected (G) and *wwtr1*-MO injected (H and I). Arrows indicate bilateral ventral aorta (H and I). (Branchial) aortic arch vessels are either reduced and/or dysplastic in *wwtr1* morphants. Arrowhead marks thyroid follicle on a (branchial) aortic arch artery of morphant larvae (I). Scale bar = 200 µm. AA, (branchial) aortic arch artery; AA1, first (branchial) aortic arch artery; AA2, second (branchial) aortic arch artery; AA3, third (branchial) aortic arch artery; AA4, fourth (branchial) aortic arch artery; HA, hypobranchial arch artery; OFT, outflow tract; ORA, opercular artery; VA, ventral aorta. Anterior is to the top in ventral view.

Table 1. Thyroid follicle number, raw diameter length of follicle lumen and follicle cell number in taz-deficient and control larvae. Number and size of thyroid follicles immunostained with the anti-TG antibody, and the number of thyroid follicle cells that were decorated for *tg* mRNA (cytoplasm) and DAPI (nuclei), were measured manually at light and confocal laser microscopy, respectively. M, mean; M_{tf}, mean thyroid follicle diameter length (µm); M_t, mean thyroid diameter length (µm); NL, number of larvae individually analyzed; P, *p*-value; SD, standard deviation.

	Control MO	***wwtr1*-MO**	**Control MO**	***wwtr1*-MO**
		3 dpf		**5 dpf**
Mean number of thyroid follicles				
NL	25	19	17	15
M	4,44	2,05	5,23	3,86
SD	1,85	1,77	2,07	1,24
P	0,000096		0,35	
Mean raw diameter length of thyroid follicles and thyroid gland				
NL	20	15	17	15
M_{tf}	11,85	8,28	15,12	13,49
SD	7,74	4,50	10,83	8,10
P	0,0069		0,31	
M_t	52,75	22,15	121,38	52,17
SD	11,04	10,55	51,46	14,11
Mean number of thyroid follicle cells (4 dpf)				
NL	10	10		
M	35,2	24,8		
SD	2,5	5,1		
P	0,0000125			

Figure 1

Click here to download high resolution image

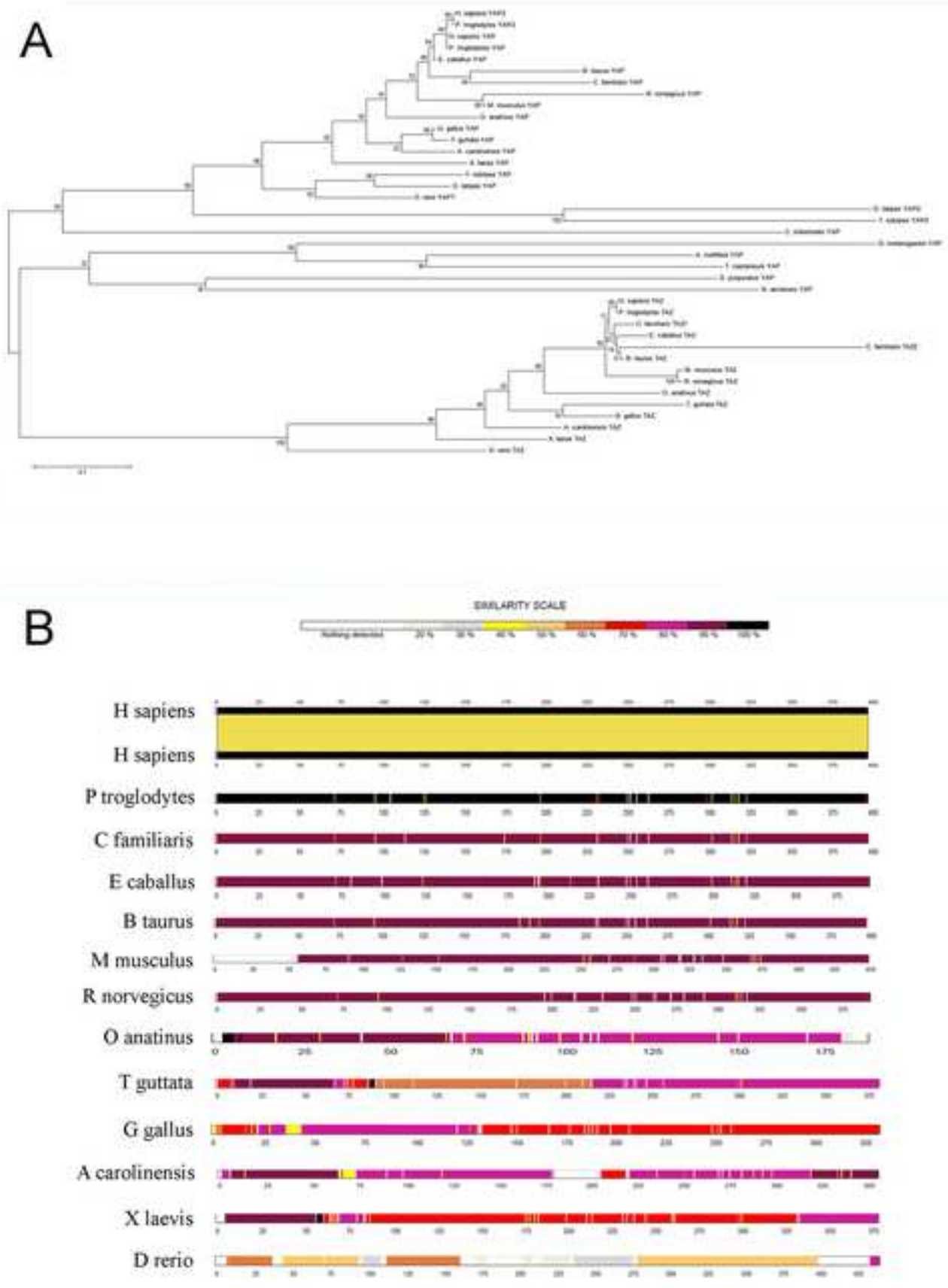

Figure 2

Click here to download high resolution image

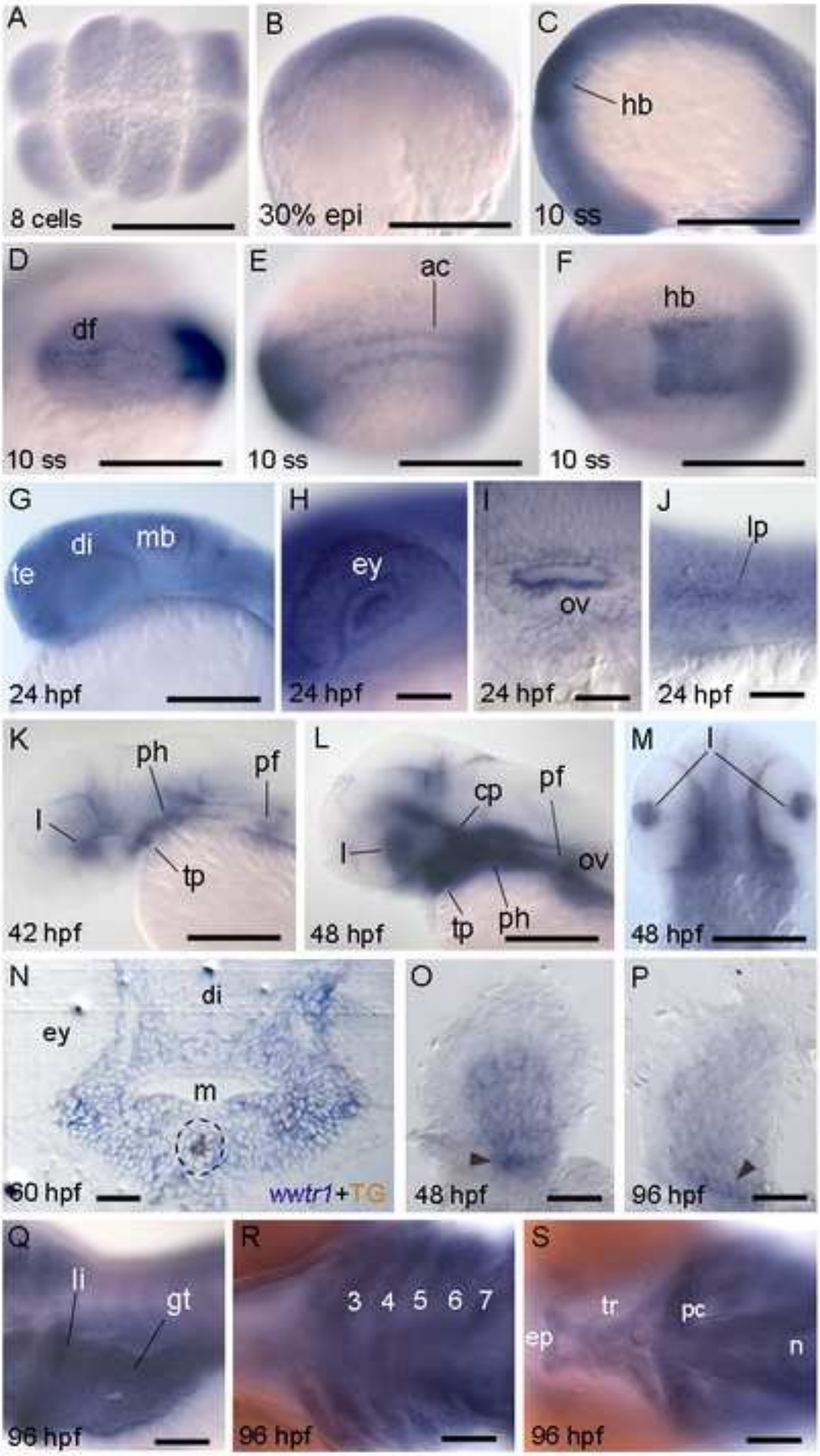

Figure 3

Click here to download high resolution image

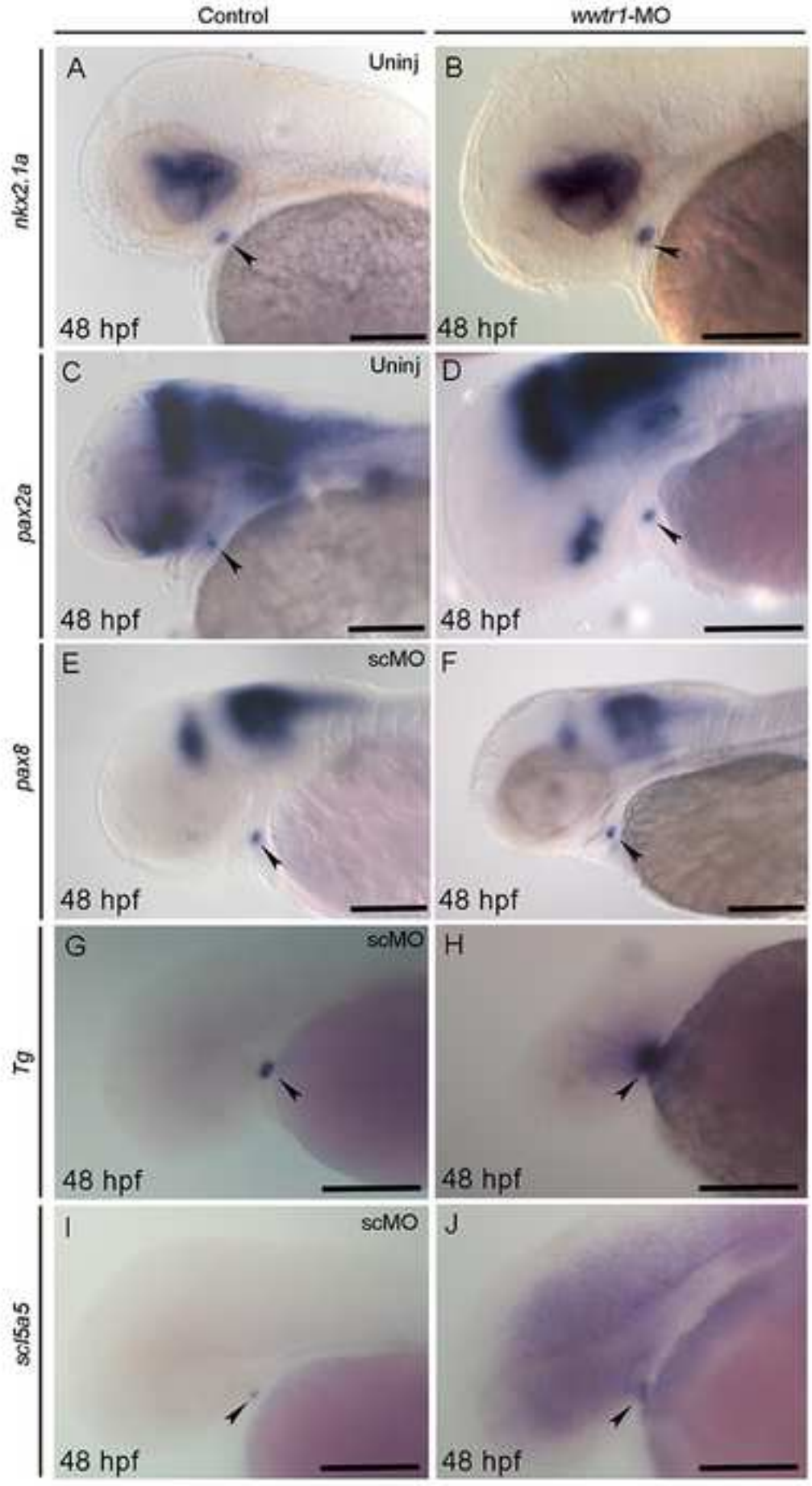

Figure 4

Click here to download high resolution image

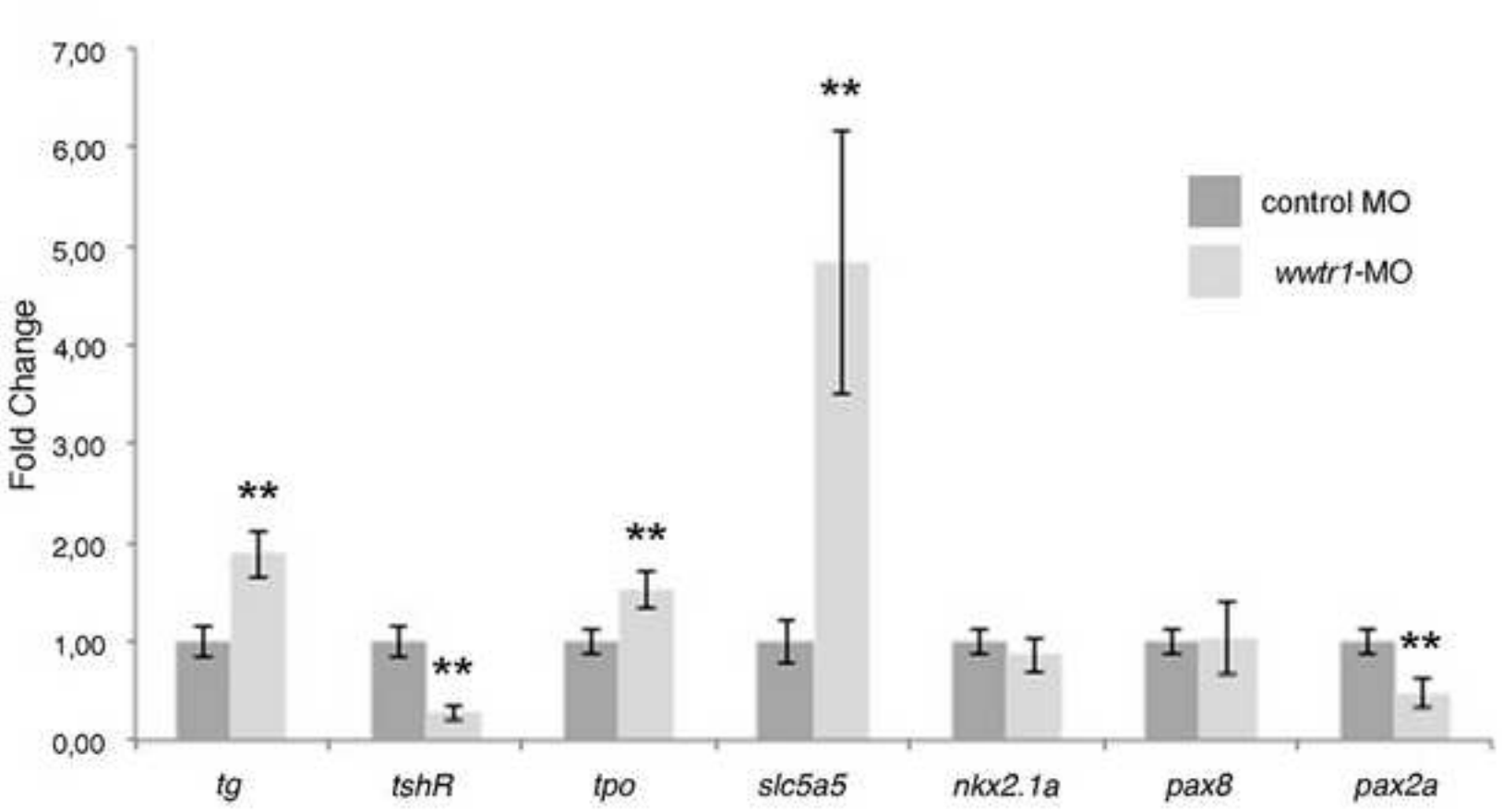

Figure 5

Click here to download high resolution image

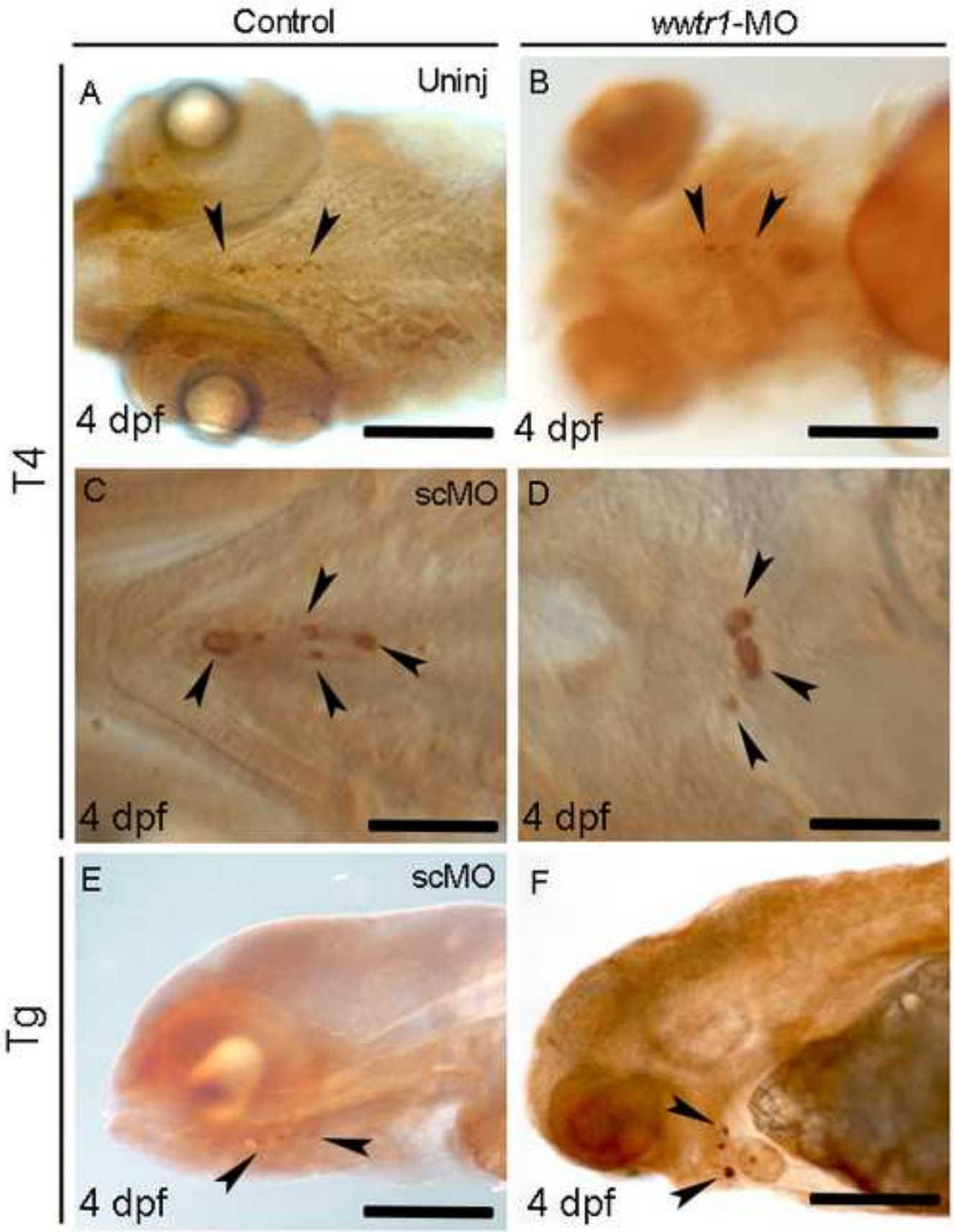

Figure 6

Click here to download high resolution image

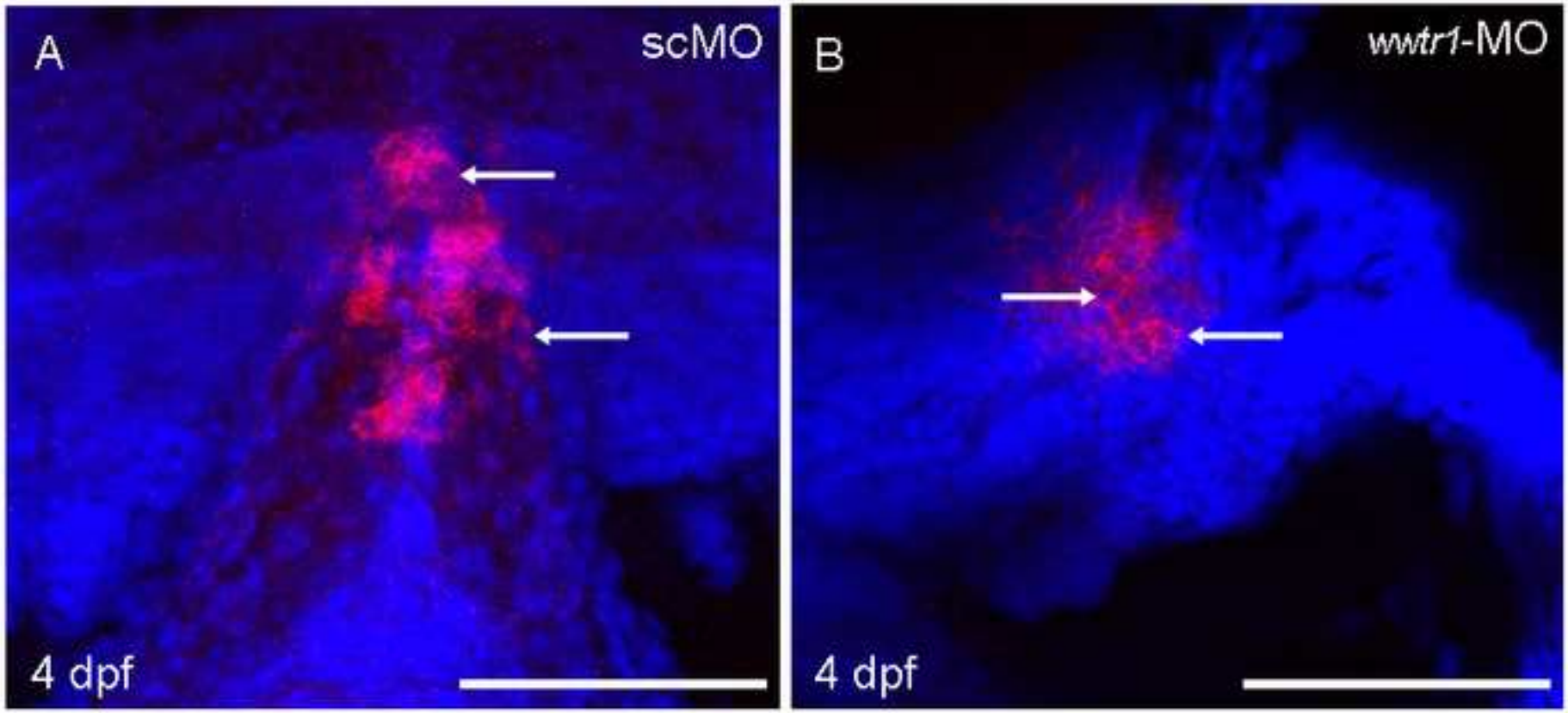

Figure 7

Click here to download high resolution image

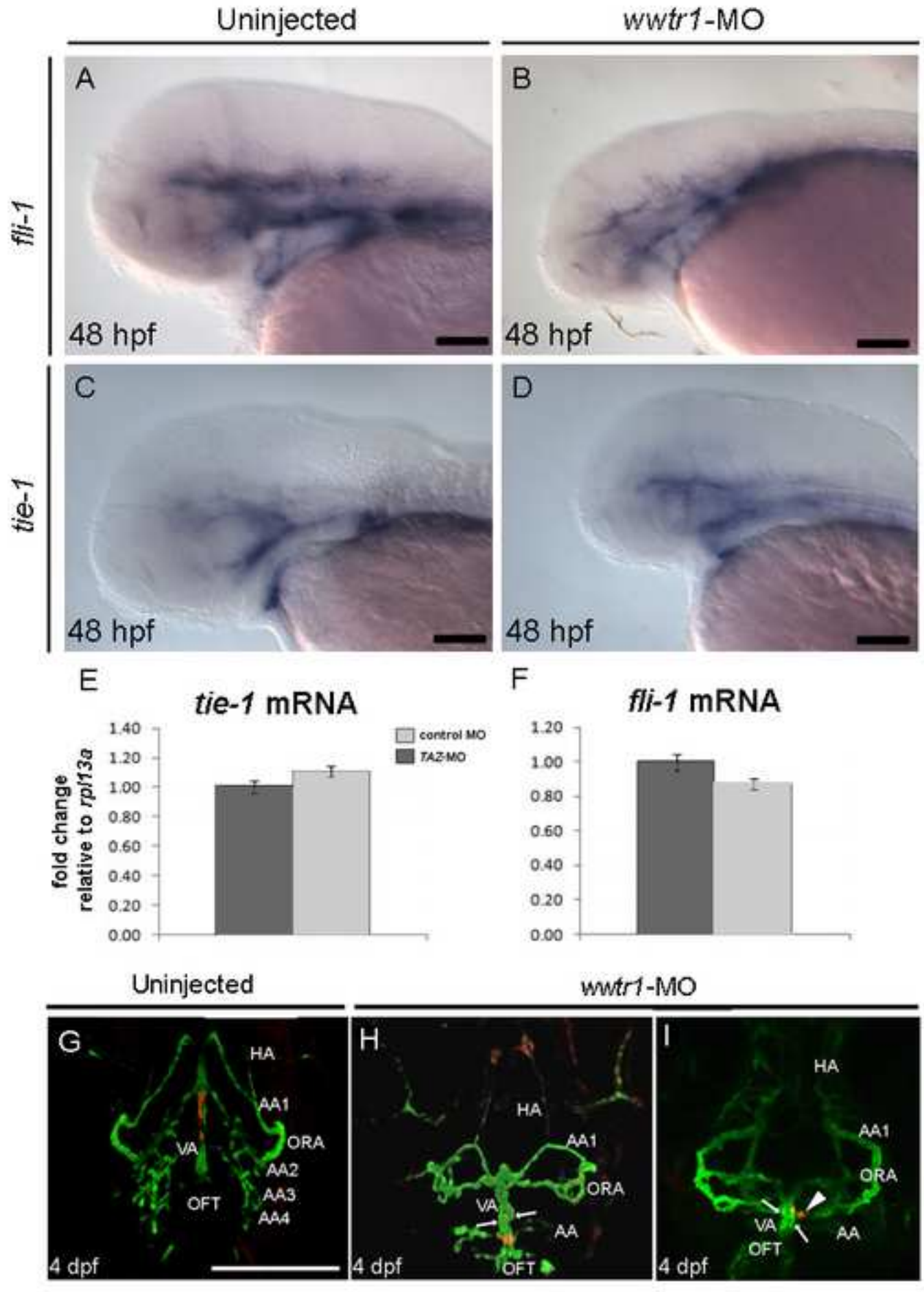

Supplemental Video 1

Click here to download Supplemental material (Multimedia Files): SupplVideo1_Pappalardo.avi

Supplemental Video 2

Click here to download Supplemental material (Multimedia Files): SupplVideo2_Pappalardo.avi